LLNL-POST-628812

# Comparison of BOUT Simulations of Drift Resistive Ballooning Turbulence to Measurements in the Edge of DIII-D L-mode Discharges

Bruce I. Cohen
Lawrence Livermore National Laboratory
Livermore, CA 94551

in collaboration with

Maxim Umansky, William Nevins, and Mike Makowski
Lawrence Livermore National Laboratory
Livermore, CA 94551

Jose Boedo and Dmitry Rudakov, UC San Diego, San Diego, CA

George McKee and Zheng Yan
University of Wisonsin-Madison, Madison, Wisconsin

Rich Groebner and DIII-D Collaboration, General Atomics
La Jolla, CA

This work was performed under the auspices of the U.S. Department of Energy by Lawrence Livermore National Security, LLC, Lawrence Livermore National Laboratory under Contract DE-AC52-07NA27344

# Comparison of BOUT Simulations of Drift Resistive Ballooning Turbulence to Measurements in the Edge of DIII-D L-mode Discharges

1. **Introduction -- Overview, definitions of suite of BOUT simulations and equations used**
2. **BOUT simulations of shot #119919 (with Te & with/without Ti fluctuations)**
3. **Plunging probe data for shot #119919 and comparison to BOUT simulation**
4. **BES data for shot #119919, GKV software synthetic diagnostic adjustment for spatial resolution of BES, and comparison to BOUT simulation**
5. **Inclusion of model $E_{radial}(r)$ fitted to probe and CER data in BOUT simulations of #119919: sheared $E_{radial}xB$ is stabilizing**
6. **Summary of comparisons between BOUT and experimental data from probe and BES for shot #119919**
7. **Simulations of colder, lower density shot #119934, with and without $E_{radial}$**
8. **New results from LAPD simulation with/without Reynolds stress zonal flow**
9. **Conclusions**

# BOUT Simulations of Resistive Drift Ballooning Turbulence in Edge Region for DIII-D L-Mode Shots #119919/..21/..30/..34

- Simulations of electromagnetic resistive drift ballooning in DIII-D L-mode shots #119919, 119921 119930, and 119934, with full geometry and magnetic shear, crossing the separatrix
- Nonlinear BOUT equations for ion density, vorticity, electron and ion velocities, electron and ion temperatures, Ohm's law, and Maxwell's equations.
- In earlier work, we have suppressed a spatial odd-even numerical mode that balloons along field line
- **Simulation results for various physics models and validation against probe and BES data**
- **BOUT obtains steady-state turbulence with fluctuation amplitudes and transport that compare reasonably to DIII-D probe and BES data. Sheared rotation due to $E_{radial}(r)$ is stabilizing, at least linearly.**

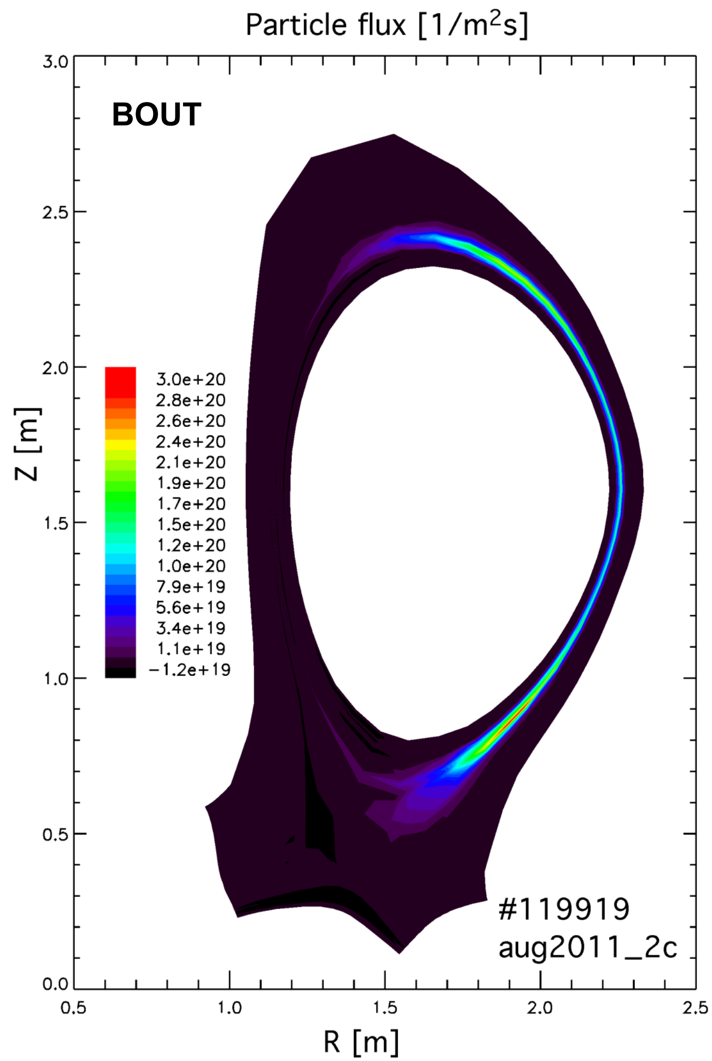

# BOUT Simulation of Resistive Drift Ballooning Turbulence for DIII-D L-mode Shots - Outline

- Electromagnetic simulations of resistive ballooning turbulence in single-null DIII-D geometry (Braginskii equations + drift ordering):
  - **Case #1:** No $T_e$ fluctuations, (**a**) with $E_r$
  - **Case #2:** With $T_e$ fluctuations
  - **Case #3:** With $T_e$ fluctuations and electron parallel thermal conduction
  - **Case #4:** With $T_e$ fluctuations, electron parallel thermal conduction, and $\nabla_{\|} = \mathbf{b}_0 \cdot \nabla + \tilde{\mathbf{b}} \cdot \nabla$ in $-\nabla_{\|}\phi$ and $\nabla_{\|} j_{\|}$
  - **Case #5:** With $T_e$ and $T_i$ fluctuations, etc.
  - **Case #6:** With $T_e$ and $T_i$ fluctuations,etc., and imposed (**a**) $E_r$ & (**b**) $5E_r$
- Comparison to probe and BES data for DIII-D shots #119919,21,30,34. These shots are well-characterized L-mode shots exhibiting steady-state turbulence.

# Case #5: Include Nonlinear Advection of $T_{e,i}$ in BOUT06 Equations for Resistive Drift Ballooning with Magnetic Flutter

- Consider the following simplified Braginskii + reduced Maxwell eqns with drift ordering in the BOUT06 framework:

$$\frac{d\tilde{N}_i}{dt} + \nabla N_i \tilde{V}_\parallel = \left(\frac{2c}{eB}\right) b_0 \times \kappa \bullet (\nabla \tilde{P}_e - N_i e \nabla \varphi) + \nabla_\parallel (\tilde{j}_\parallel / e)$$

$$\frac{d\varpi}{dt} = 2\omega_{ci} b_0 \times \kappa \bullet \nabla \tilde{P} \quad + \quad N_{i0} Z_i e \frac{4\pi V_A^2}{c^2} \nabla_\parallel \tilde{j}_\parallel$$

$$\frac{d\tilde{V}_{\parallel e}}{\partial t} = -\frac{e}{m_e} E_\parallel - \frac{1}{N_{i0} m_e} (T_{e0} \nabla_\parallel \tilde{N}_i) + 0.51 \nu_{ei} \tilde{j}_\parallel$$

$$\frac{d\tilde{V}_{\parallel i}}{dt} = -\frac{1}{N_{i0} M_i} \nabla_\parallel \tilde{P},$$

$$\frac{d\tilde{T}_{e,i}}{dt} = \frac{2}{3N_{i0}} \nabla \bullet \left( \kappa_\parallel^{e,i} \nabla_\parallel \tilde{T}_{e,i} \right), \quad \kappa_\parallel^e = 3.2 \frac{N_{i0} T_{e0} \tau_{e0}}{m_e}, \ \kappa_\parallel^i = \ldots$$

$$\mathbf{E} = -\frac{\mathbf{1}}{c}\frac{\partial}{\partial t}\mathbf{A}_\parallel - \nabla \varphi, \quad -\nabla_\perp^2 \mathbf{A}_\parallel = \frac{4\pi}{c} \mathbf{j}_\parallel, \quad \mathbf{B} = \nabla \times \mathbf{A}_\parallel + \mathbf{B}_0$$

$$\varpi = \nabla \cdot \left[ e Z_i N_i \nabla \varphi \right] + \nabla_\perp^2 P_i \approx e Z_i N_{i0} \nabla^2 \varphi \qquad \nabla_\parallel = \mathbf{b}_0 \cdot \nabla + \tilde{\mathbf{b}} \cdot \nabla \quad Z_i = 1$$

$$\frac{d}{dt} = \frac{\partial}{\partial t} + (\mathbf{V}_{E0} + \tilde{\mathbf{V}}_E) \bullet \nabla \quad N_i = N_{i0} + \tilde{N}_i, \quad T_s = T_{s0} + \tilde{T}_s, \ldots$$

$$\tilde{P} = N_{i0}(\tilde{T}_e + \tilde{T}_i) + \tilde{N}_i (T_{e0} + T_{i0}), \quad T_{i0} = T_{e0}, \quad V_{\parallel s0} = 0$$

- Electromagnetic with
  $\nabla_\parallel = \mathbf{b}_0 \cdot \nabla + \tilde{\mathbf{b}} \cdot \nabla$ in $-\nabla_\parallel \phi$ and $\nabla_\parallel \tilde{j}_\parallel$
- Actual DIII-D geometry
- Radial bdry conditions: Von Neumann on fluid fluctuations, Dirichlet on $A_\parallel$ & $\phi$

  Fluctuations decay to 0 at outer bdry & not necessarily at inner bdry
- DIII-D - like fixed background profiles for shots #119919 and 119934
- Case #4 includes $T_e$ fluctuations (not $T_i$ fluctuations) and parallel heat conduction
- Case #5 includes all of the above

*B. Cohen, et al., APS DPP 2012*



Fusion Energy Sciences

# History of rms fluctuation amplitudes in midplane at separatrix with electron parallel thermal conduction and magnetic flutter, showing saturated turbulence in BOUT for shot #119919

**BOUT Cases 4 and 5**

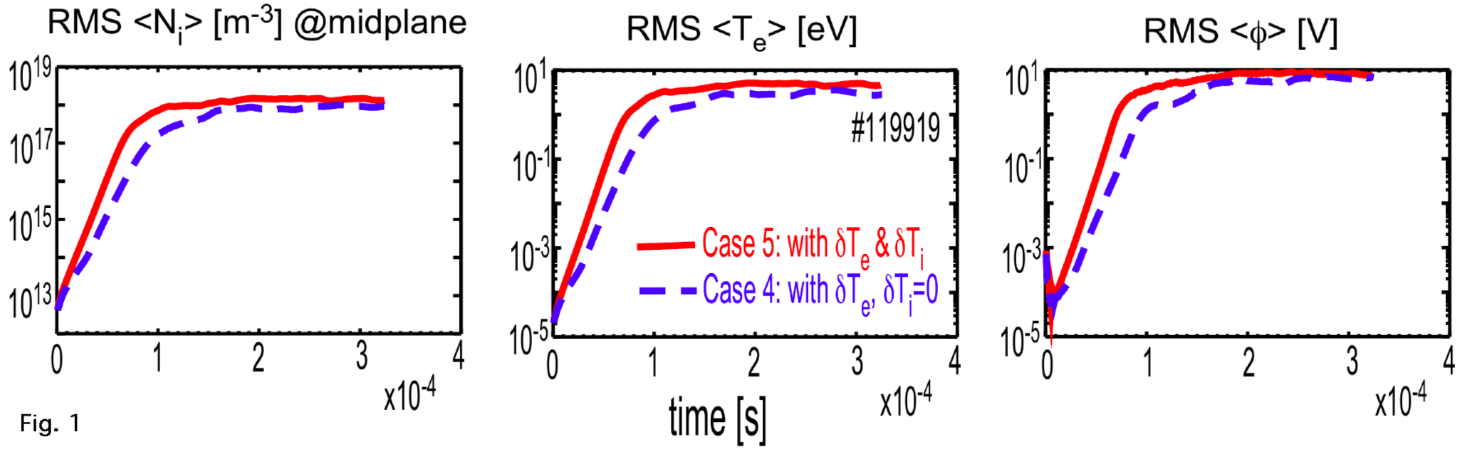


Fig. 1

- With $T_e$ (& $T_i$) fluctuations, electron parallel thermal conduction, convective nonlinearities, and

$$\nabla_{\parallel} = \mathbf{b}_0 \cdot \nabla + \tilde{\mathbf{b}} \cdot \nabla \text{ in } -\nabla_{\parallel}\phi \text{ and } \nabla_{\parallel} j_{\parallel}$$

- Temperature and density fluctuations saturate

- Including $T_i$ fluctuations increases fluctuation amplitudes modestly

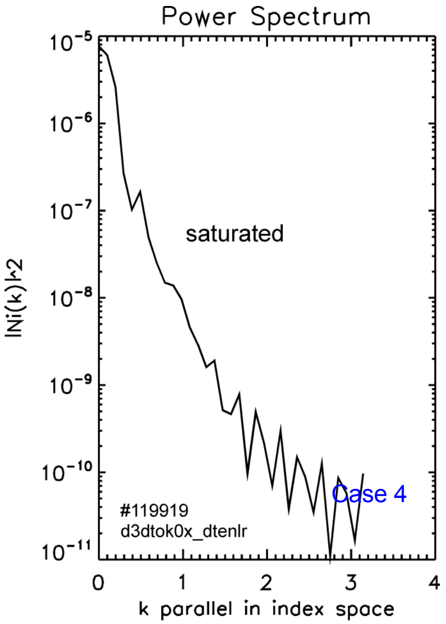


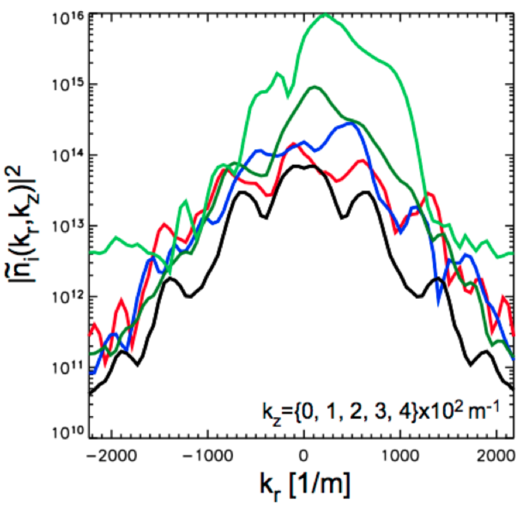


Fig. 9

*B. Cohen, et al., APS DPP 2012*

# Time-averaged ion density fluctuations in the midplane saturate at ~10-30% and peak near $R_{sep}$

**BOUT Cases 4 and 5**

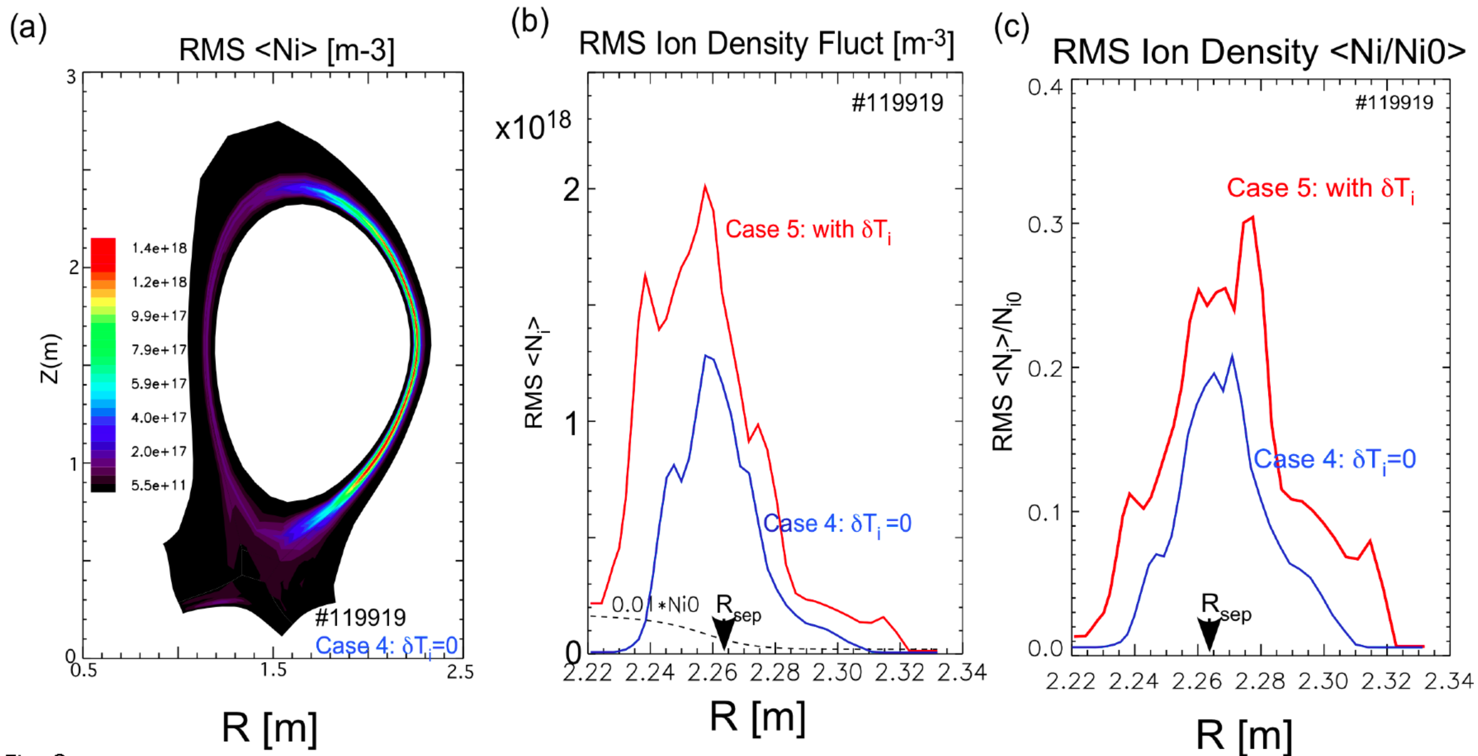


Fig. 2

- With $T_e$ fluctuations, electron parallel thermal conduction, and $\nabla_{\parallel} = \mathbf{b}_0 \cdot \nabla + \tilde{\mathbf{b}} \cdot \nabla$
- Including $T_i$ fluctuations leads to higher fluctuation amplitudes
- There is a poloidal asymmetry wrt midplane in the fluctuations

*B. Cohen, et al., APS DPP 2012*

# Ballooning Nature of Turbulence, Case 1 #119919

**BOUT Case 1**

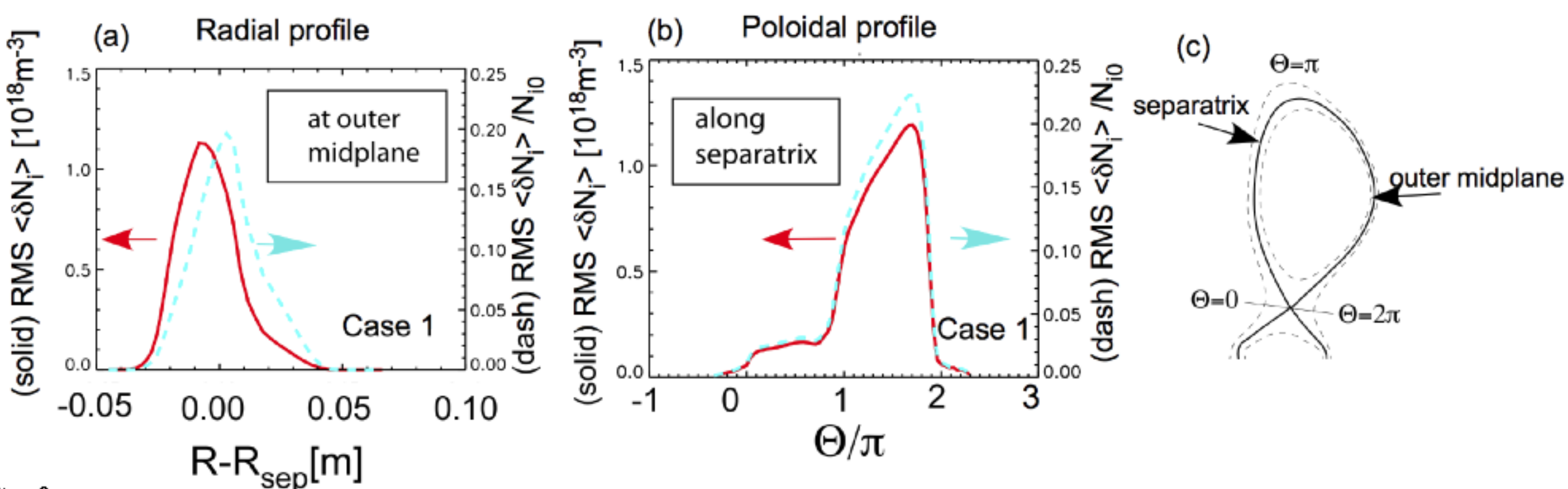


Fig. 6

- The fluctuations are radially localized near the separatrix
- The fluctuations balloon to the outer side of torus where the pressure-weighted curvature drive is strongest

*B. Cohen, et al., APS DPP 2012*

# Time-averaged $T_e$ fluctuations in the midplane peak near the $R_{sep}$ and saturate at ~50-150% relative amplitude at $R>R_{sep}$

**BOUT Cases 4 and 5**

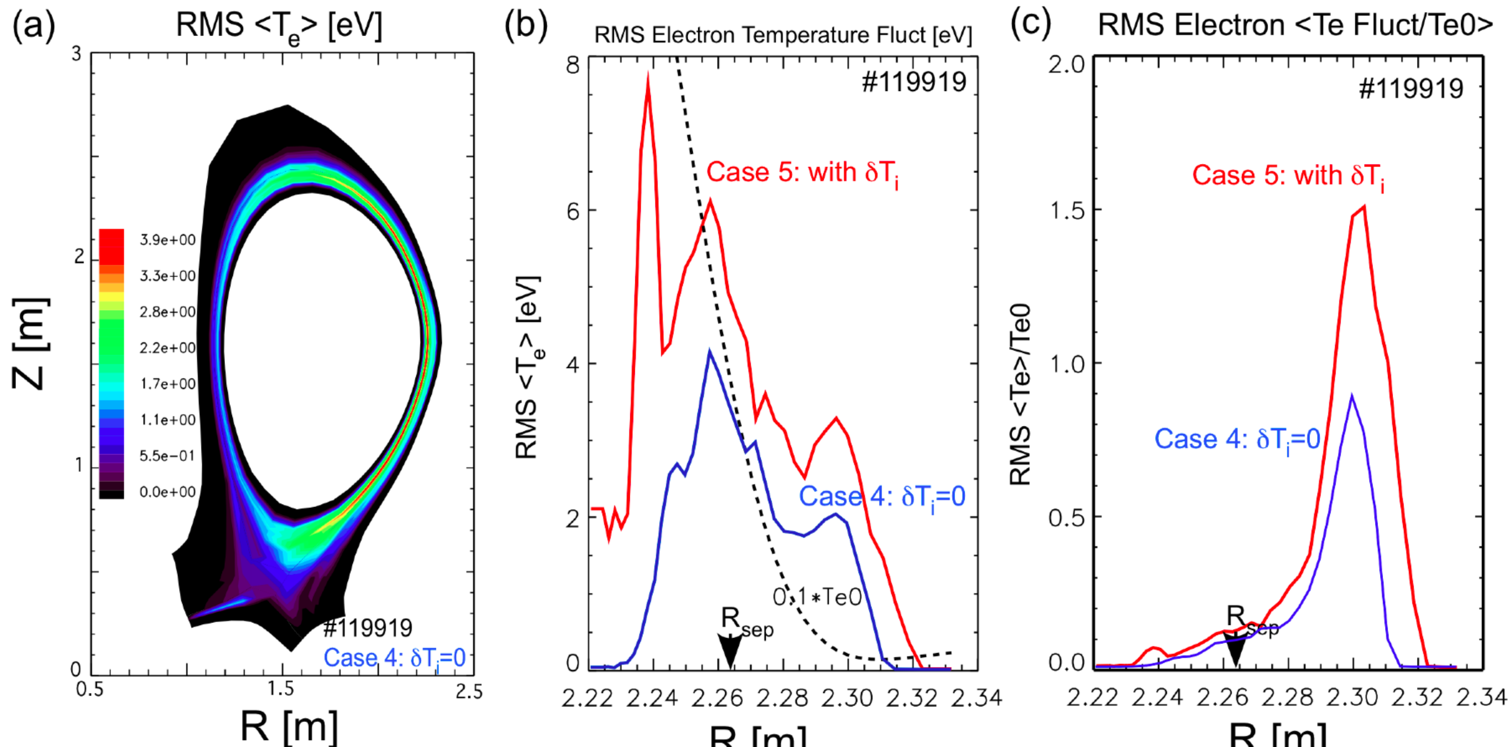


Fig. 3

- With $T_e$ fluctuations, electron parallel thermal conduction, nonlinear convection, and $\nabla_{\parallel} = \mathbf{b}_0 \cdot \nabla + \tilde{\mathbf{b}} \cdot \nabla$
- $T_e$ fluctuations are ~10% near $R_{sep}$ and are higher with finite $T_i$ fluctuations

*B. Cohen, et al., APS DPP 2012*

# Time-averaged ion particle diffusion coefficient in the midplane saturates at ~1.5-2 $m^2/s$

**BOUT Cases 4 and 5**

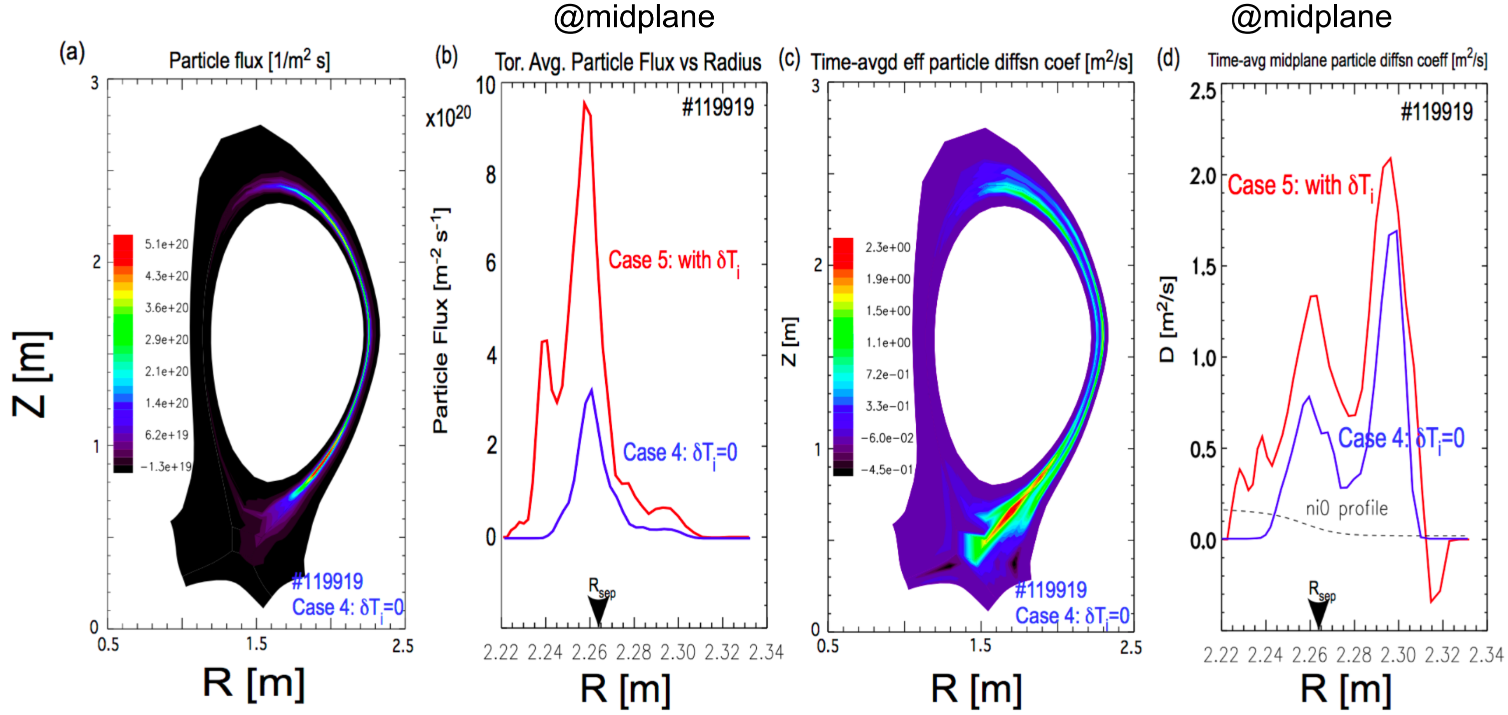


- With $T_e$ fluctuations, electron parallel thermal conduction, nonlinear convection, and $\nabla_{\parallel} = \mathbf{b}_0 \cdot \nabla + \tilde{\mathbf{b}} \cdot \nabla$
- Including $T_i$ fluctuations leads to higher particle fluxes and diffusion coefficient

*B. Cohen, et al., APS DPP 2012*

# Time-averaged electron conductive thermal diffusion coefficient in the midplane saturates at ~2-6 m²/s

**BOUT Cases 4 and 5**

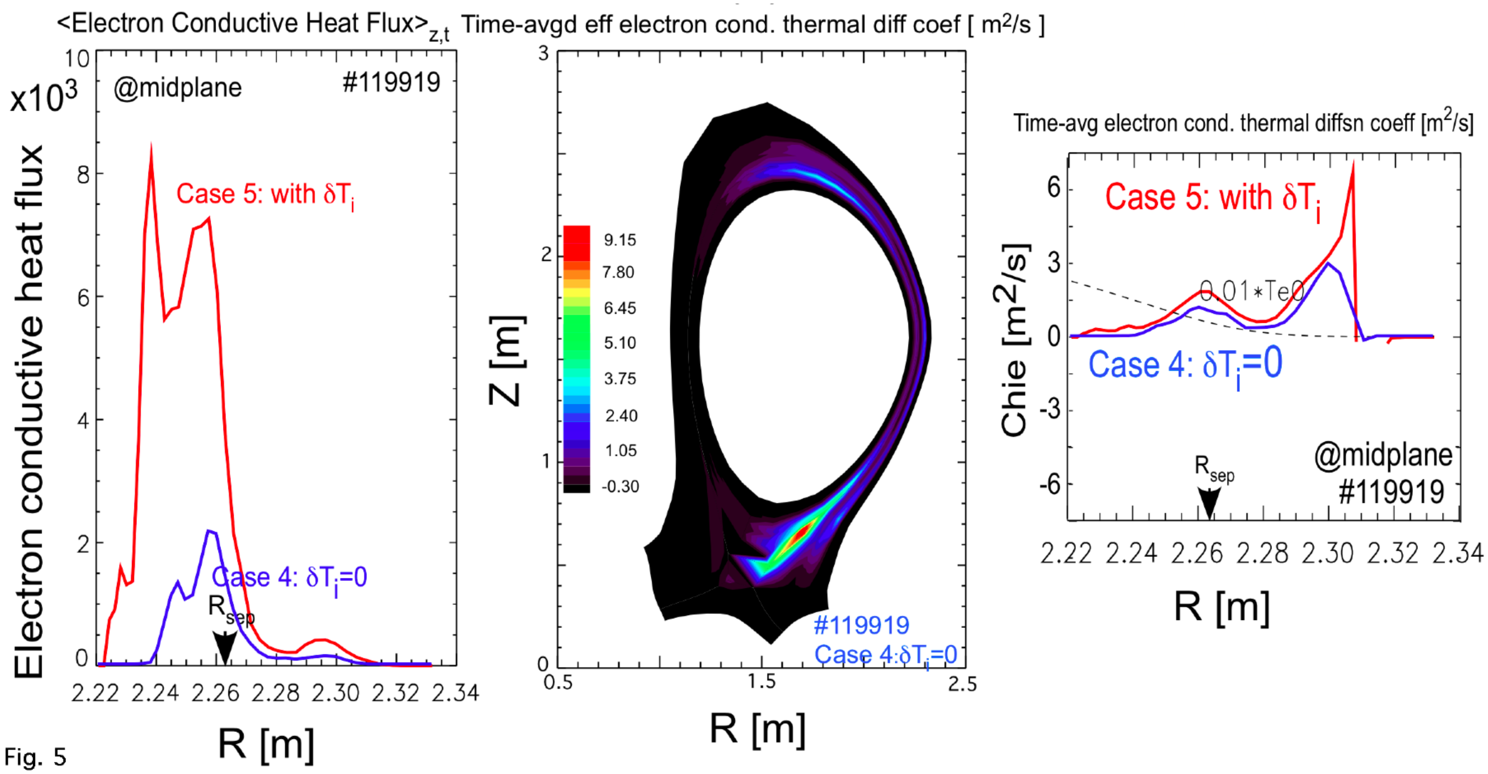


Fig. 5

Note: Here heat flux (conductive) = $\frac{3}{2}N_0 < \delta v_r \delta T_e >_{tor,t}$, and $\chi_e = -\frac{3}{2}N_0 < \delta v_r \delta T_e >_{tor,t} / N_0 \nabla T_{e0}$

- With $T_e$ fluctuations, electron parallel thermal conduction, nonlinear convection, and $\nabla_{\parallel} = \mathbf{b}_0 \cdot \nabla + \tilde{\mathbf{b}} \cdot \nabla$
- Including $T_i$ fluctuations leads to higher heat fluxes and diffusion coefficient

# There is reasonable agreement between BOUT simulation and Langmuir probe data for DIII-D #119919 with respect to peak fluctuation amplitudes, particle and thermal flux, and localization

- BOUT with $T_e$ & $T_i$ fluct'ns, electron parallel thermal conduction, convective nlrity, $\nabla_{\parallel} = \mathbf{b}_0 \cdot \nabla + \tilde{\mathbf{b}} \cdot \nabla$

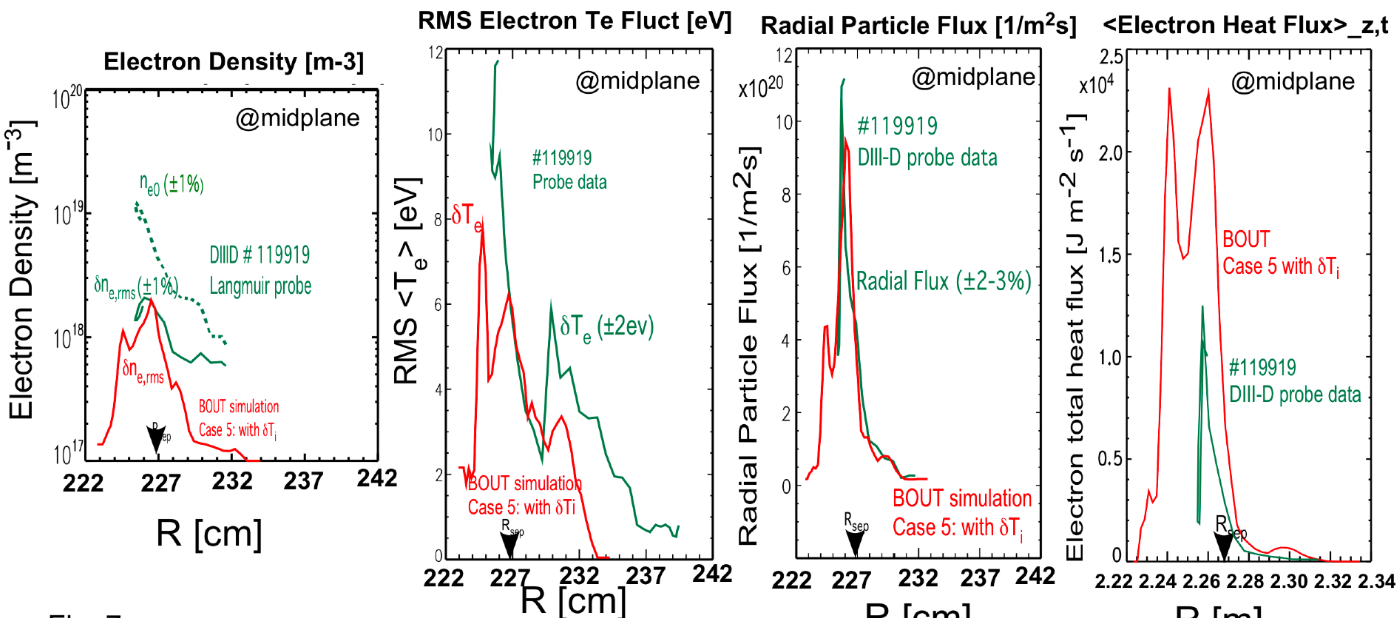


Fig. 7

**Radius at midplane→**

- Probe signals decrease below noise levels for R > 231 cm, and stop for R < 225 cm
- Typical experimental rms $\delta n_e$ and $\delta T_e$ fluctuations at the separatrix exceed ~20% & ~50%
- $\delta n_e$, $\delta T_e$ and the probe fluxes in the midplane usually peak near the separatrix
- BOUT simulations and Langmuir probe data agree within factors of 2 in peak amplitudes and localization for 2.25m ≤ R ≤ 2.31m

*B. Cohen, et al., APS DPP 2012*

# BES Measurements: Long-Wavelength Density Fluctuation Characteristics in 119921-- G. McKee, Z. Yan

- Short beam-blips injected to obtain BES data during L-mode plasma conditions

**BES 4x4 Grid**

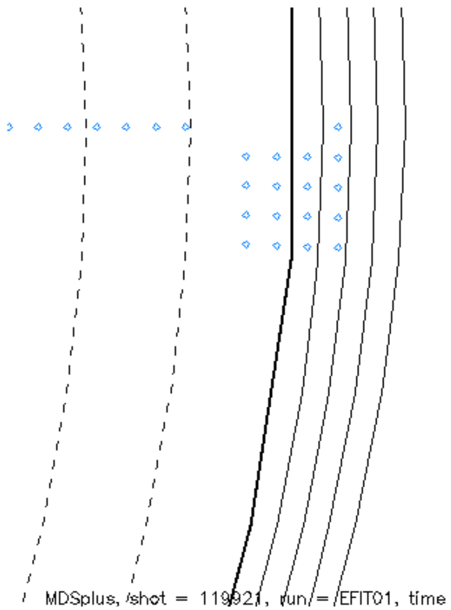


**Density Fluctuation Spectrum**

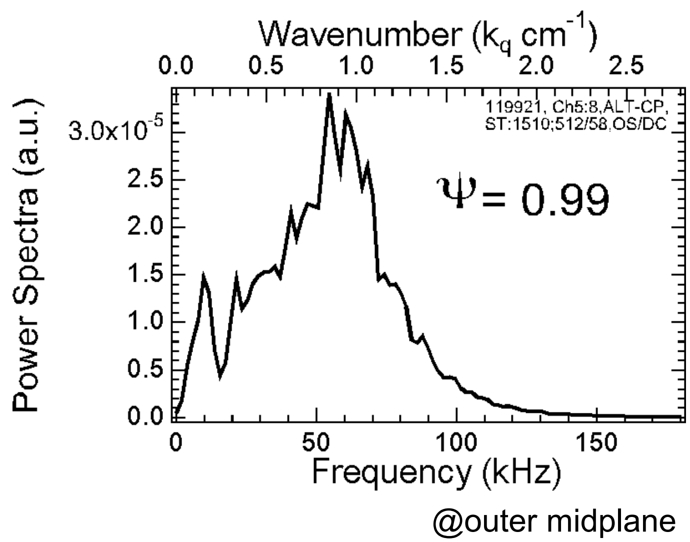


**(Preliminary Analysis)**

**$\tilde{n}$/n Amplitude Profile**

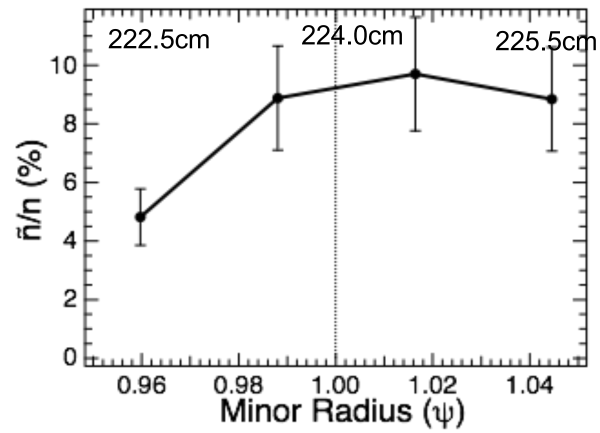


**Spatial Correlation**

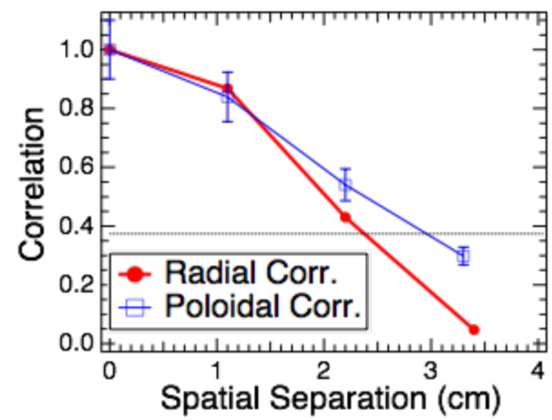


*B. Cohen, et al., APS DPP 2012*

# Synthetic Simulation Diagnostics Using GKV Suite to Match BES Data

- GKV is a suite of IDL routines built by Bill Nevins to analyze data from simulations or experiments. GKV includes routines to compute various quantities of interest, e.g., power spectra vs. *k* or $\omega$ or ($\omega$, *k*); correlation functions, etc., and various plots.

  refs: W.M. Nevins, "GKV User's Manual", UCRL-TR-206016 (Aug. 2004); W.M. Nevins *et als*., Phys. Plasmas **13**, 122306 (2006).

- We construct synthetic diagnostics using the GKV suite of IDL routines to compare to BES data. Spatial filtering (1D or 2D) required in simulation diagnostics to model the Δx=1 cm limit on spatial resolution in the BES grid in R and Z. Filtering is applied to both the radial and binormal coordinates thru the convolution

$$f_{smooth}(x) = \int dx' w(x-x') f(x'), \text{ where } w(x) = \begin{cases} \frac{1}{2\Delta x}\left[1+\cos\left(\frac{\pi x}{\Delta x}\right)\right] & \left|\frac{x}{\Delta x}\right| < 1 \\ 0 & \left|\frac{x}{\Delta x}\right| > 1 \end{cases}$$

- Correlation functions are defined by normalized integrals:

$$C(f;x,t) = \frac{\iint dx'\, dt'\, f(x',t')\, f(x'-x,t'-t)}{\iint dx'\, dt'\, f(x',t')\, f(x',t')}$$

- We construct synthetic diagnostics using the GKV suite to compare to BES data. Spatial filtering (1D or 2D) is required in simulation diagnostics to model the 1 cm limit on spatial resolution in the BES grid in R and Z.

# Reasonable Agreement between BOUT Simulation and Beam Emission Spectroscopy Data for DIII-D #119921 with respect to Peak Fluctuation Amplitude, Localization, Spatial Correlation Width, and Spectral Width

**ñ/n Amplitude Profile**

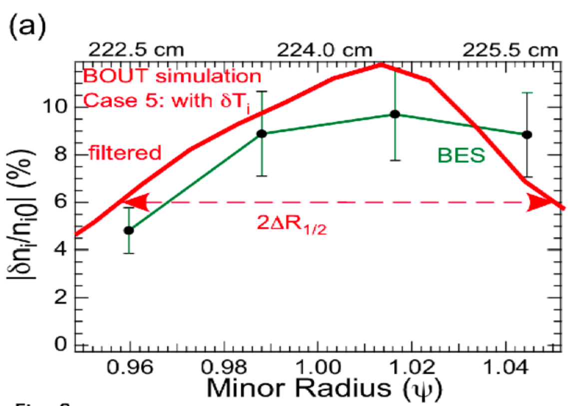


**Spatial Correlation**

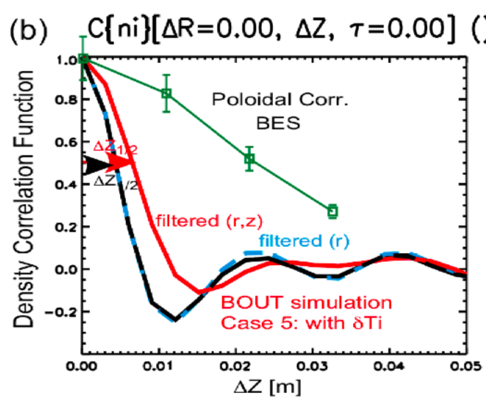


**Density Fluctuation Spectrum**

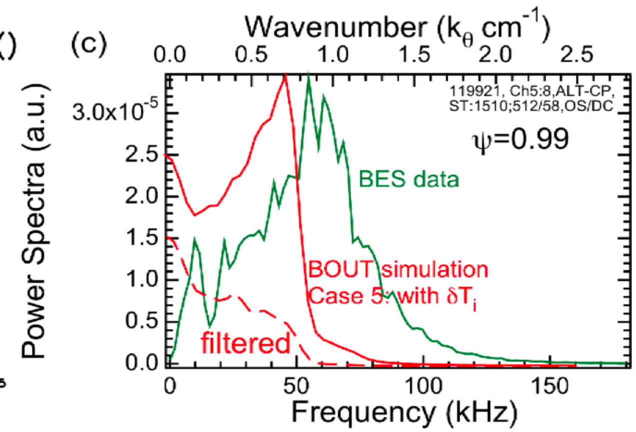


@outer midplane

- Spatial filtering of the BOUT diagnostics reduces and spatially spreads peaks
- There is agreement between BOUT and BES to within factors of two or three, or better

# Philosophy on the Modeling of Sheared Radial Electric Field and Zonal Flow Effects

- Sheared ExB flows can reduce linear growth rates and saturated turbulence levels for drift-type instabilities, e.g., core ITG, L-H transition phenomenology,…
- But zonal flows are not always important, e.g. in the ETG study of Holland et al., Nuc. Fusion **43**, 761 (2003), zonal flows are not an important feature.
- In the edge, $E_r(r)$ is influenced by sheaths at the divertor plates and limiters, by interactions with neutral gas, sources/sinks, other non-ambipolar processes, and the turbulence-generated zonal flows via the Reynolds stress.
- If there is good experimental data for $E_r(r)$ that is sufficiently resolved spatially and temporally, and extends over the whole spatial domain, this data would incorporate all the physics to determine the zonal flows completely.
- We first study the effects of (1) an imposed steady $E_r(r)$ based on fitting to experimental data and (2) $E_r(r,t)$ including the Reynolds stress for all modes except for the longest radial wavelengths of the axisymmetric modes which are held constant at their initial defined values to maintain "equilibrium" profiles (ref. Waltz & Candy).

# Model the Experimental Radial Electric Field to Study the Effects of Imposed $E_0$xB Shearing on Simulated Turbulence

- An equilibrium radial electric field $E_0$ is included in BOUT simulations for Cases 1, 4, & 5, using fits to the experimental probe and CER data near the midplane
- L-mode plasmas typically have weakly sheared ExB flows. In our fit to probe and CER data the ExB shearing rate is < 2.4 x $10^4$ (1/s) < BOUT growth rates~O(1)x$10^5$(1/s)
- We expect that with imposed sheared ExB flow there will be weaker linear instability and some reduction of the saturated turbulence

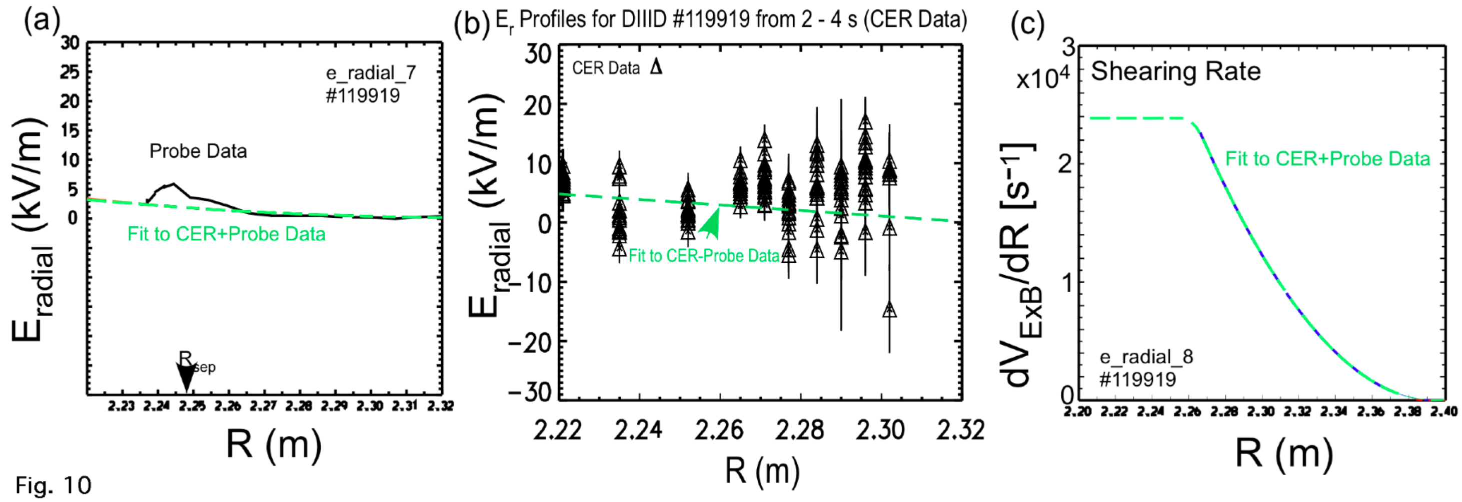


Fig. 10

*B. Cohen, et al., APS DPP 2012*

# Imposed $E_0$xB Shearing Reduces Both Linear Growth Rates and Saturated Turbulent Amplitudes

- An equilibrium radial electric field $E_0$ is included in BOUT simulations for #119919 **Cases 1, 4, 5, & 6**, using fits to the experimental probe and CER data near midplane
- In our fit to probe and CER data the ExB shearing rate is < 2.4 x $10^4$ (1/s) < BOUT growth rates~O(1)x$10^5$(1/s)
- Imposed sheared ExB flow weakens linear growth rates, and saturation is much delayed (>2ms) and at lower amplitudes, while 5x$E_r$ is much more stabilized.

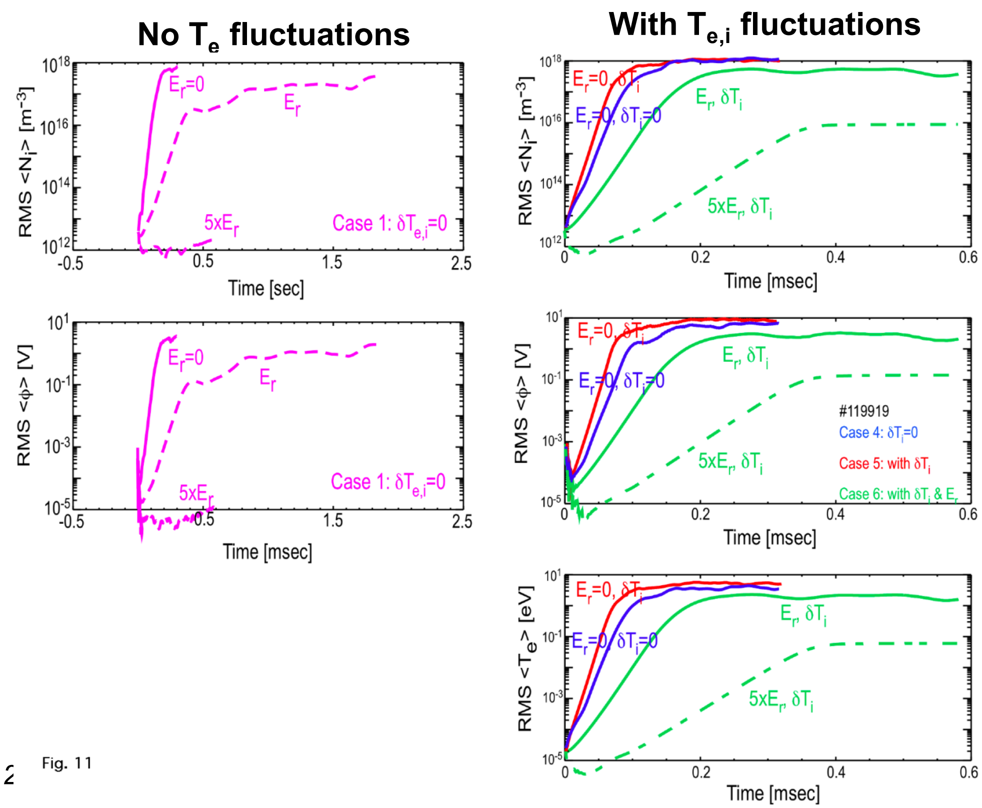


Fig. 11

*B. Cohen, et al., APS DPP 2*

# Imposed $E_0$xB Shearing Reduces Both Linear Growth Rates and Saturated Turbulent Amplitudes in Simulations

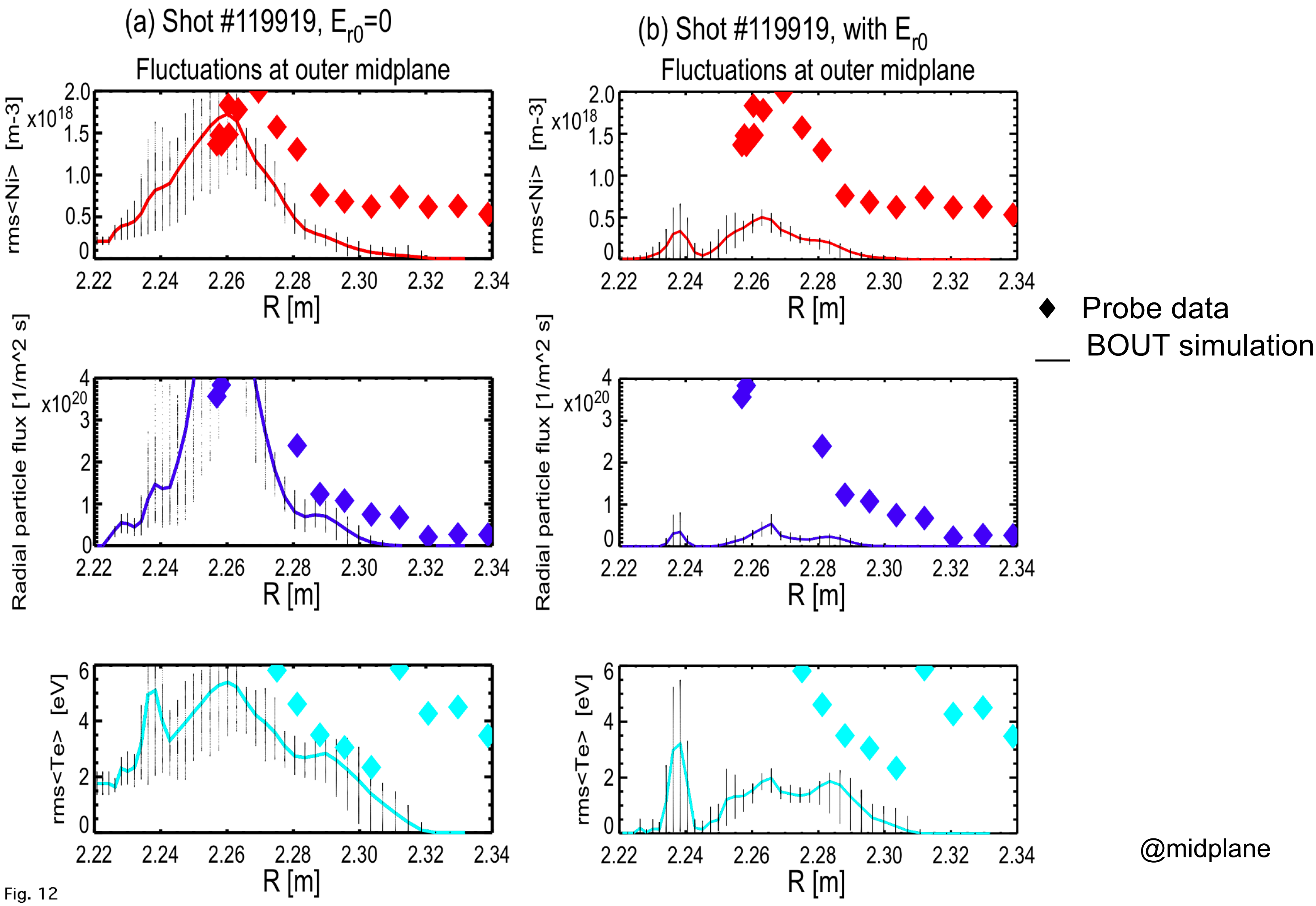


Fig. 12

*B. Cohen, et al., APS DPP 2012*

# As the Physics Model Becomes More Complete, the Agreement of BOUT Results with DIII-D Probe Data Improves - Summary

- Comparison of suite of BOUT simulations to shot #119919: peak values in midplane at saturation near $R_{sep}$ ($E_{rad}$=0, $E_{rad}\neq 0$, $E_{rad}=5E_{rad}$ with $\delta T_e$ convective nonlinearity)

| Bout simulation | $<\delta N_i>_{rms}$ ($10^{18}\ m^{-3}$) | $<\delta T_e>_{rms}$ (eV) | Radial Particle Flux ($10^{20}\ /m^2\ s$) | $D_r$ ($m^2/s$) local | Conductive Radial Heat Flux $=\frac{3}{2}N_0 < \delta \tilde{v}_r \delta \tilde{T}_e >$ ($10^3\ J/m^2\ s$) | $\chi_e$($m^2/s$), local (conductive) |
|---|---|---|---|---|---|---|
| **#1**: $\delta T_e=0$<br>#1a: w/$E_r$** | 0.95<br>0.37 | N/A<br>N/A | 1.8<br>0.07 | 0.4<br>0.02 | N/A<br>N/A | N/A<br>N/A |
| **#4**: $\delta T_e\neq 0$<br>$\kappa_{\|\|e}\neq 0$ & $\tilde{\mathbf{b}}\cdot\nabla$ | 1.3 | 4.0 | 3.3 | 1.7 | 3.3 | 2.7 |
| **#5** & w/$\delta T_i$ | 2.0 | 7.5 | 9.5 | 2 | 10 | 2.2 |
| **#6a** w/$E_r$<br>**#6a** w/5$E_r$ | 0.7<br>0.3 | 5.5<br>3.5 | 0.8<br>0.18 | 0.27<br>0.035 | 2.5<br>0.75 | 0.32<br>0.036 |
| DIII-D #119919 probe data | 2.0 | 10 | 11.0 | ~0.2-1 ‡ | 1.2 | ~1-2 ‡ |

**Cases #1 w/$E_r$ has not saturated at end of simulation (1.8 ms)

‡Typical, flux-surface-averaged values for shot #119919 inferred from UEDGE reconstruction

# Comparison of BOUT Results with BES Data for Suite of Physics Models - Summary

- Comparison of suite of BOUT simulations to shot #119921 BES data: fluctuation frequency spectra, peak density amplitude radial half-width, correlation lengths
- Factor of 2 or better agreement seen between simulation synthetic diagnostics with filtering and the DIII-D #119921 BES data (with or without sheared $E_0 xB$ velocity included in BOUT)

| Bout simulation | $\langle \delta N_i/N_i \rangle_{rms}$ peak vs. R raw/filtered | $\Delta R_{half\text{-}max}$ of $\langle \delta N_i/N_i \rangle_{rms}$ (cm) raw/filtered | $\Delta Z_{corr,half\text{-}max}$ of density (cm) raw/filtered | Peak freq in density fluct't'n spect, raw/filtered ($10^5$ rad/s) | Freq half-max in density fluct't'n spect, raw/filtered ($10^5$ rad/s) |
|---|---|---|---|---|---|
| **#1**: $\delta T_e=0$ | 0.13 / 0.07 | 1.2 / 1.5 | 0.6 / 0.9 | 3 / 0.5 | 4 / 2 |
| **#1a**: w/$E_r$** | 0.065/0.045 | 0.7/0.8 | 2.0 / 2.3 | 0 / 0 | 1/ 0.7 |
| **#4**: $\delta T_e \neq 0$ $\kappa_{\|e} \neq 0$ & $\tilde{\mathbf{b}}\cdot\nabla$ | 0.20 / 0.12 | 1.4 / 1.2 | 0.4 / 0.7 | 3.0 / 1.5 | 2 / 1.2 |
| **#5**: w/$\delta T_i$ | 0.21 / 0.12 | 1.7 / 2 | 0.4 / 0.7 | 3.0 / 0&1.5 | 1 / 1.5 |
| **#6a**: w/$E_r$ | 0.07 / 0.05 | 1.5 / 1.7 | 0.8/ 0.9 | 0.5 / 0.5 | 0.5 / 0.5 |
| **#6b**: $E_r$=5$E_r$ | 0.011/0.006 | 0.5 / 0.6 | 3/3 | 3.8 / 3.8 | 0.25 / 0.25 |
| DIII-D #119921 BES data | 0.09 ±0.2 | 2 ±0.2 | 2 ±0.2 | 3.8 | 1.3 ±0.2 |

**Cases #1 w/$E_r$ has not saturated at end of simulation (1.8 ms)

*B. Cohen, et al., APS DPP 2012*



Fusion Energy Sciences

# Comparison of Probe Data from Shots #119930 and 119934 vs. 119919 -- Edge Plasmas with Lower Density and Temperature

- L-mode shots #119930 and 119934 edge plasmas are colder and have lower densities than in shot #119919
- The growth rate for resistive ballooning is proportional to $\eta^{1/3}\beta^{2/3}/n^{1/3} \propto T^{1/6}n^{1/3}$
- A factor of two lower temperature and density decreases the drive for resistive ballooning by O(1/√2) if all else is fixed in shots #119930/119934 vs. #119919

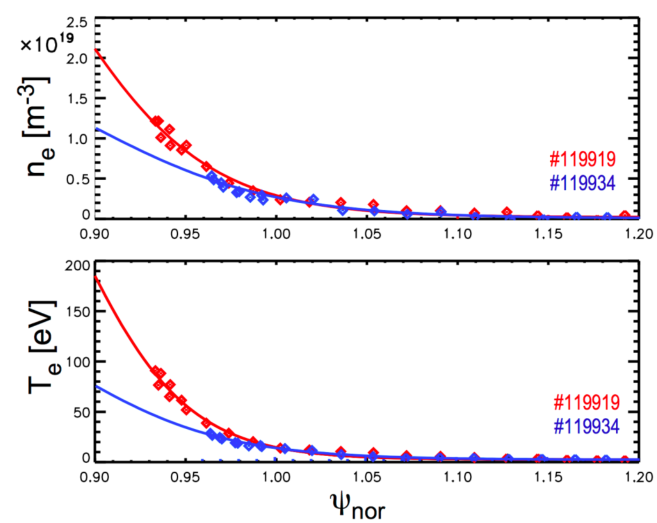


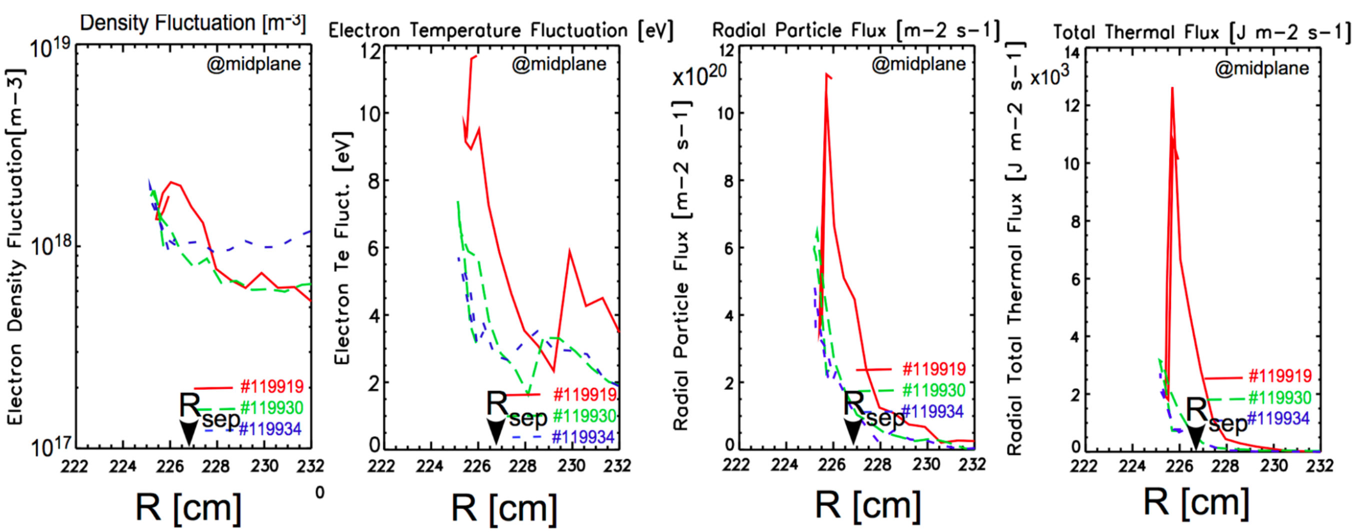


Reduced $N_{i0}$ & $T_{e0}$ lead to **reduced fluctuation amplitudes and radial fluxes** in #119930 & 119934

@midplane

*B. Cohen, et al., APS DPP 2012*

# BOUT Simulations of Shots #119919 and 119934 Show Turbulence Is Reduced at Lower Equilibrium Temperature and Density

@midplane

- BOUT simulations of **Case 5** with no $E_{radial}$ for shots # 119919 and 119934 show that the linear growth rate for the resistive-drift ballooning instability is reduced in 119934, in qualitative agreement with theoretical expectation with its lower equilibrium electron temperature and density in the edge
- The absolute values of the fluctuation amplitudes are reduced in 119934 accompanying the reduction in growth rate of the instability
- Note that cases with temperature fluctuations have increased interchange drive in general and with $T_i$ fluctuations are more unstable than without.

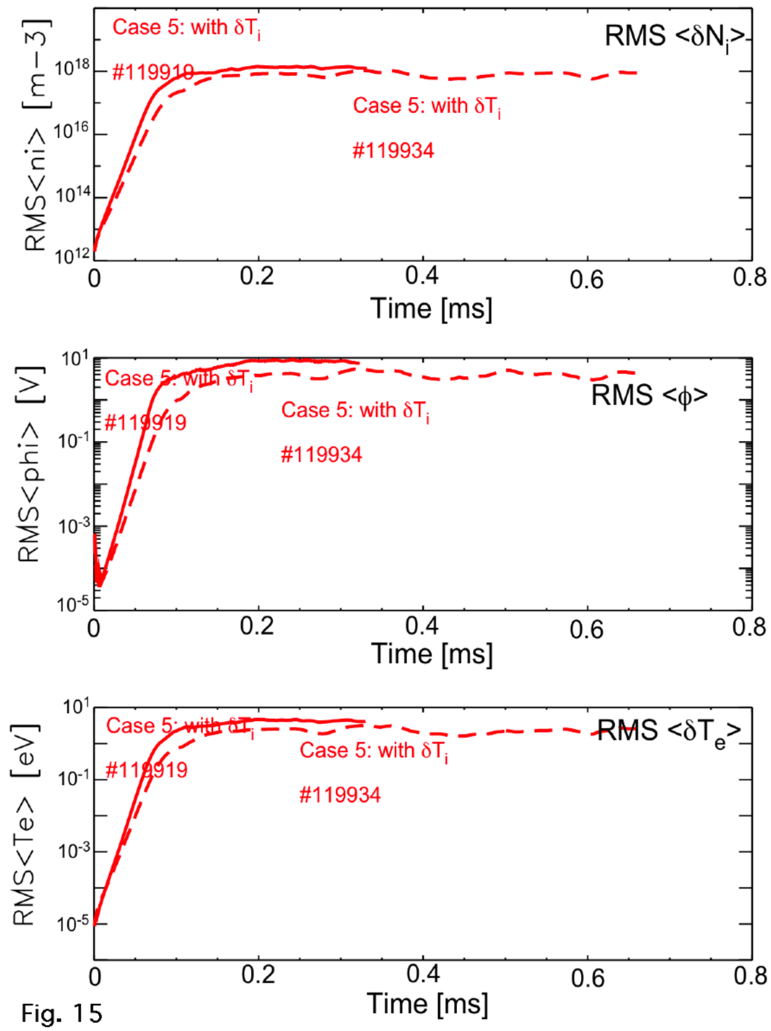


Case 5 #119919,34

Fig. 15

*B. Cohen, et al., APS DPP 2012*

# BOUT Simulation and Probe Data Show that #119934 Is Slightly Less Turbulent Than #119919

- Probe data from L-mode shots #119919 & 34 are compared with BOUT simulations including $T_e$ & $T_i$ fluctuations (**Case 5**). Turbulence in #119934 is slightly reduced from that in #119919
- Density and temperature fluctuations, and radial fluxes tend to peak near the separatrix

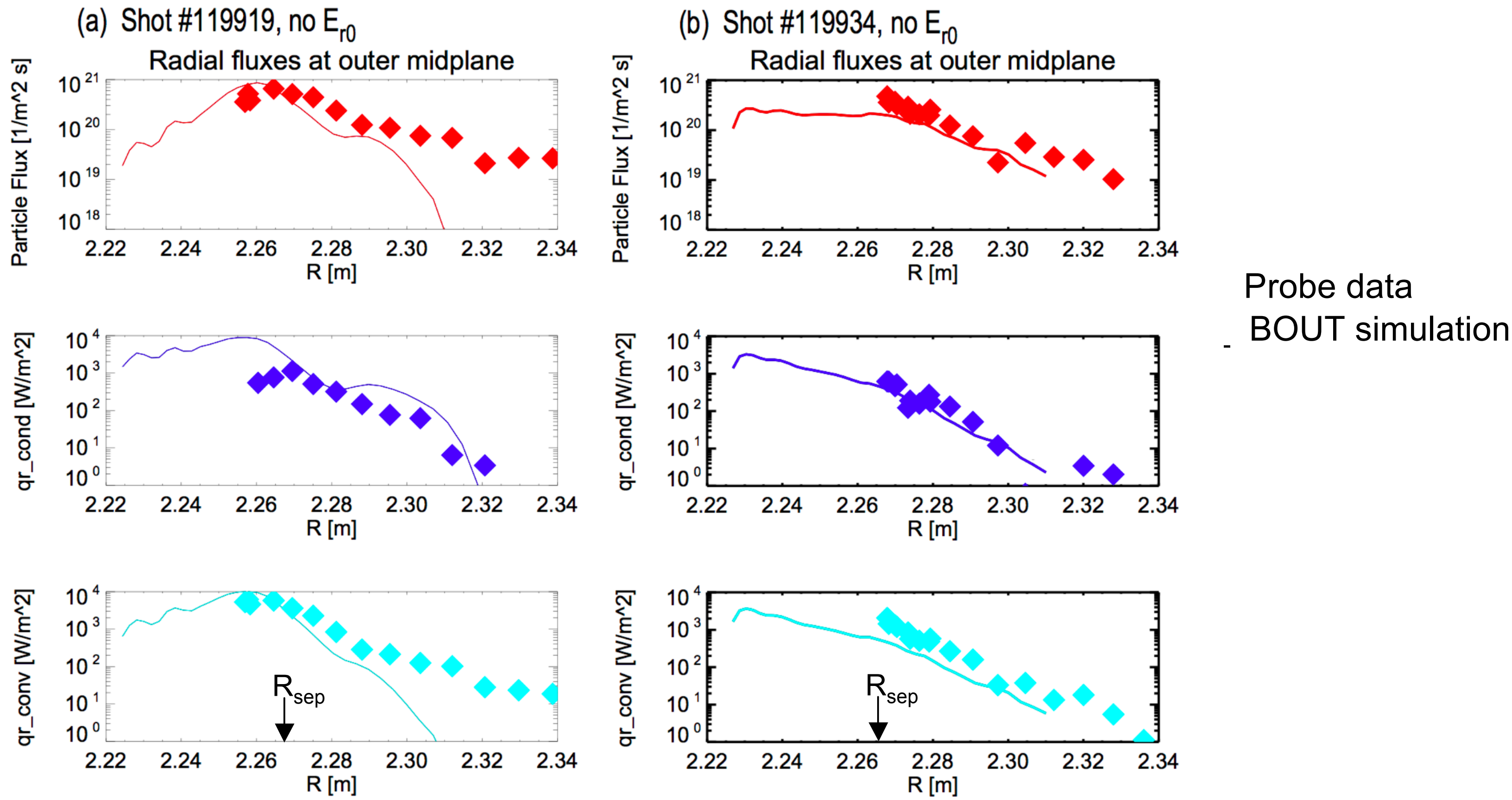


*B. Cohen, et al., APS DPP 2012*



Fusion Energy Sciences

# Radial Electric Fields Fitted to Probe and CER Data for Simulations of Shots #119919, 119930 and 119934

- The electric potential and radial electric field are well determined from the probe data in the SOL, but tend to diverge and become unreliable inside the last closed flux surface
- The radial electric field determined by CER extends to smaller radii and shows that $E_{radial}$ is relatively flat within significant temporal scatter

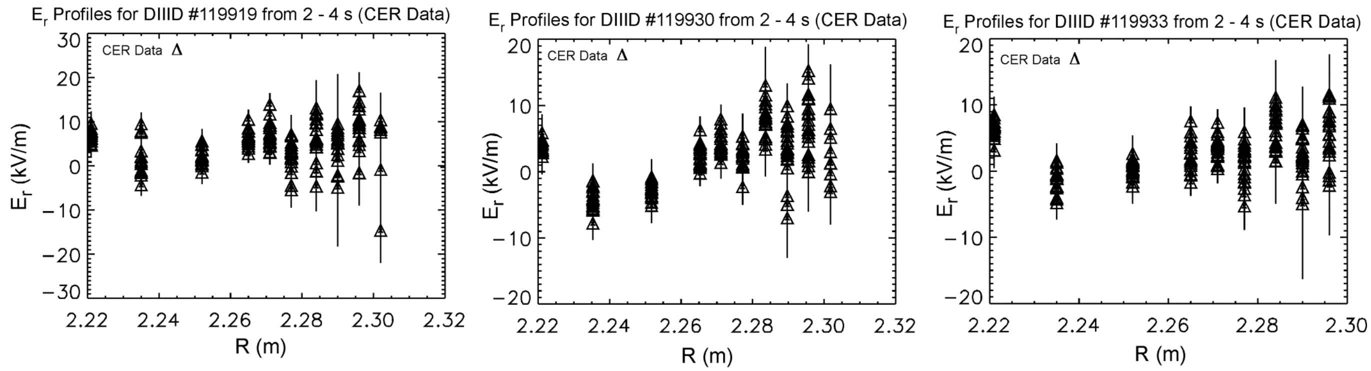


$E_{radial}$ CER data

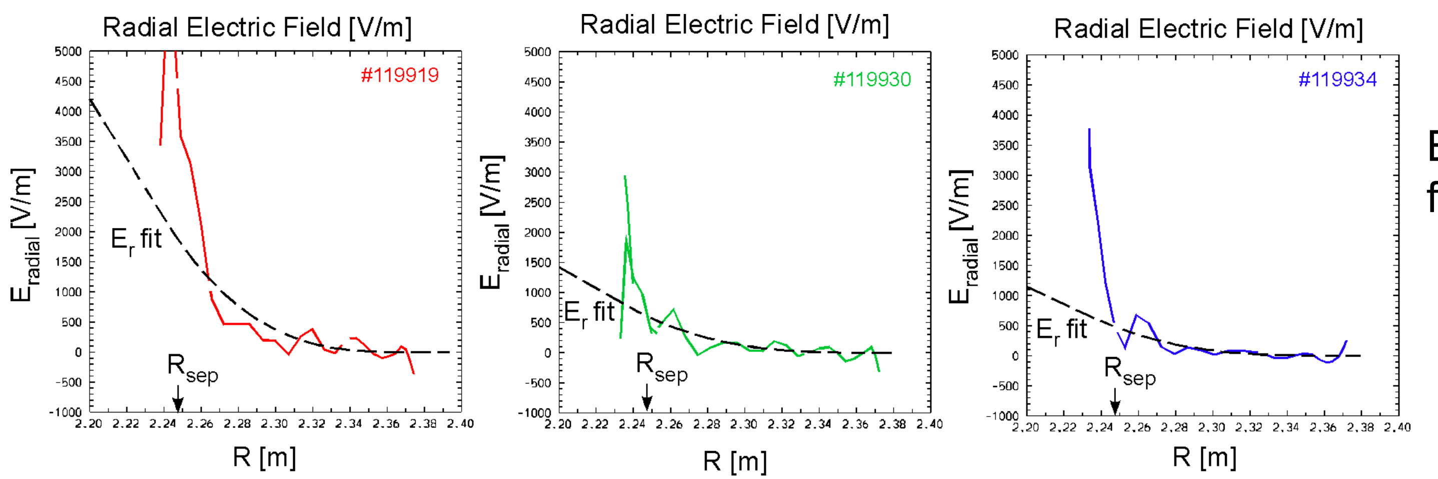


$E_{radial}$ probe data & fit to probe/CER data

*B. Cohen, et al., APS DPP 2012*

# Inclusion of Radial Electric Field Reduces Growth Rates and Saturated Fluctuation Levels in Simulation of Shot #119934

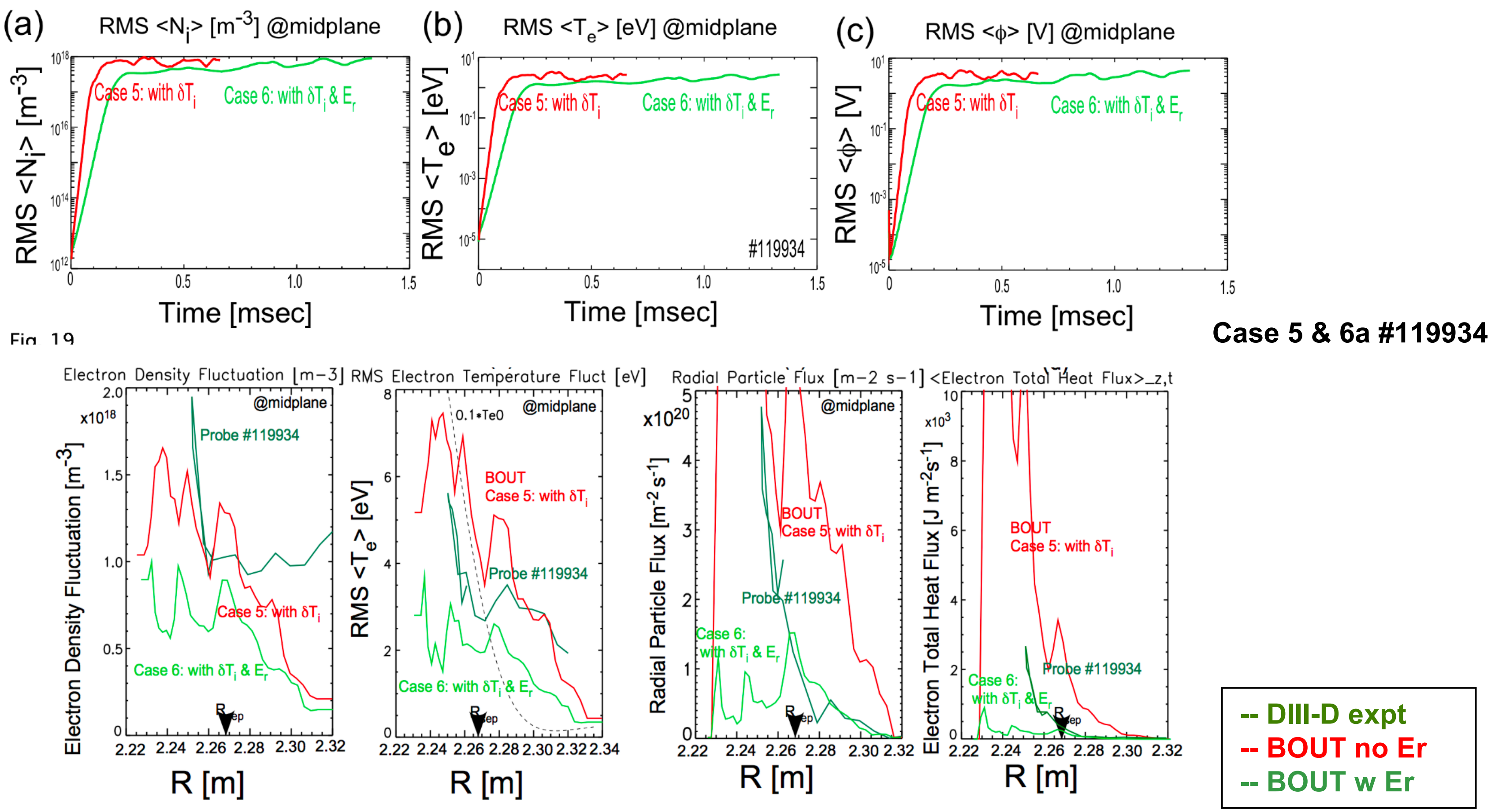


- Inclusion of $E_r$ reduces linear growth rates and saturated fluctuation amplitudes less so; the finite $E_r$ saturated amplitudes tend to recover to the levels of the $E_r$=0 case
- Simulation agreement with probe for relevant radii, 2.25m ≤ R ≤ 2.31m, remains fair

*B. Cohen, et al., APS DPP 2012*

# Evidence of Stabilizing Effects of Sheared Radial Electric Field with Reynolds Stress Zonal Flow Effects in Simulation of LAPD Edge Turbulence

- We simulate edge turbulence in LAPD cylindrical geometry with a 3-field electrostatic model supporting drift resistive instability (density, vorticity, electron temperature) including $E_r$ and the effects of the Reynolds stress on zonal flows for all modes except the longest radial wavelengths of the axisymmetric modes (which are held constant at their initial defined values to maintain “equilibrium” profiles fitting the experiment).

- We have compared simulations with imposed $E_{r0}$ and with/without the Reynolds stress zonal flow effects. The Reynolds stress reduces the saturated turbulence in the edge by a factor of 2-3 in the rms amplitudes early in the saturation. Plotted here are (a) the total electric potential $\phi_{tot}=\phi_0+\phi$ vs. radius at various times at saturation, (b) rms fluctuating $<\phi>$ at a/2 and L/2 vs. time, and (c) snapshots of the fluctuating $\phi(r,\theta)$ showing the Reynolds zonal flow effects. $\phi_0$ is from expt.

- These simulations are being extended, and DIII-D L-mode simulations will be undertaken.

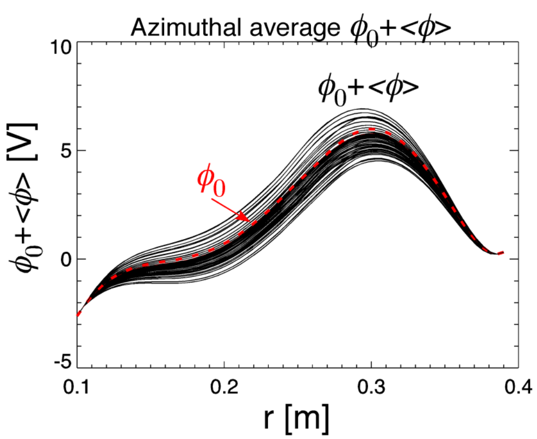


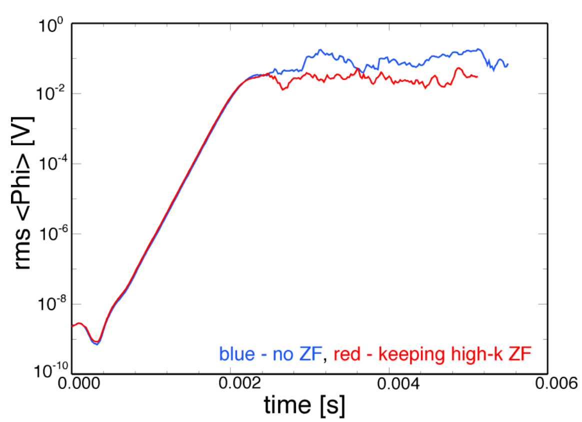


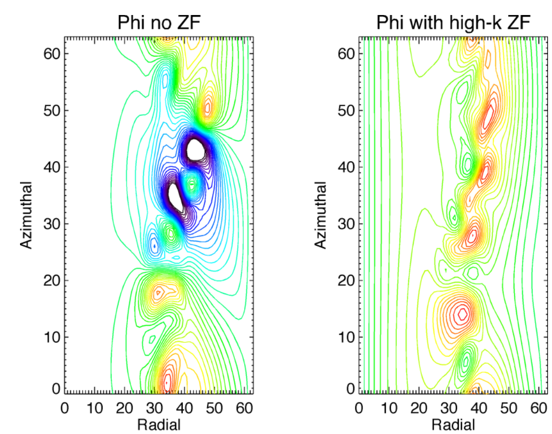


*B. Cohen, et al., APS DPP 2012*

# Summary: Relative Agreement in Comparison of BOUT Results with DIII-D Probe and BES Data on Shots #119919 & 119934

- Comparison of suite of BOUT simulations to shots #119919/119921 probe and BES data: fluctuation frequency spectra, peak density amplitude radial half-width, correlation lengths, fluxes and diffusion rates are in reasonable agreement.
- RMS peak density and temperature fluctuation amplitudes measured with the Langmuir probe agree (#119919 & 119934) within factors of 2 or better with simulations as the physics model improves. Observed radial particle diffusivities and thermal conduction diffusivities in simulation are consistent with typical L-mode inferred values.
- Spatial filtering of the synthetic simulation diagnostics is needed to model the 1 cm spatial resolution of the BES data. The spatial filtering spreads and reduces peaks in the raw data.
- There is factor-of-2 or better agreement seen between simulation synthetic diagnostics and the DIII-D #119921 BES data for the relative ion density and $T_e$ fluctuation amplitudes, particle flux, spatial widths, and spectral frequency widths.
- Inclusion of the radial $E_{radial}$ inferred from experiment introduces a weakly sheared ExB flow that reduces growth rates and saturation amplitudes in simulations. But saturated amplitudes can recover nonlinearly, e.g., #119934. Reynolds stress may reduce turbulence.
- Colder, lower density edge plasmas are less unstable and have smaller fluctuation levels.
- **Drift resistive ballooning modes are a reasonable candidate for L-mode edge plasma turbulence in DIII-D shots #119919/21, #119930/34.**